We sincerely thank the referee for the positive assessment of the scientific value and relevance of our dataset and for the constructive suggestions. We have carefully considered all the comments raised by both referees and have substantially revised the event classification, related statistical analyses, CCN evaluation, and methodological descriptions. Our point-by-point responses are provided below.

Comment 1:

I would recommend removing the distinction between NPF event Class I and Class II, and suggest these to be called NPF events. As seen from the supplement figures S1 and S2, there seem to be some days (Oct 26, March 25 and March 26) classified as Class I days, which by definition of Class I should show uninterrupted growth of particles but there are clear gaps in the measured PNSD data. On the other hand, some days (at least Oct 10 and Oct 19) seem to have quite continuous growth of particles, but these days have been classified as Class II days.

Response 1：

We thank the referee for this important suggestion. We agree that the distinction between the original Class I and Class II events was not sufficiently robust. As the referee noted, some days originally classified as Class I contained temporary gaps in the measured PNSD, whereas some Class II days exhibited relatively continuous particle growth. In addition, the similar magnitudes and diurnal variations of J_3 and J_7 between the original Class I and Class II events further indicated that maintaining two separate NPF event classes was not well justified.

We have therefore removed the Class I–Class II distinction from all main analyses and combined the two original categories into a single "NPF day" category. The revised classification now consists of NPF, Undefined, and Non-Event days. NPF days were identified primarily from the appearance of a distinct new particle mode followed by identifiable growth toward larger sizes in the daily PNSD. Continuous and uninterrupted growth throughout the entire day was not required because temporary gaps may result from changes in air masses, boundary-layer development, variations in precursor availability, or missing measurements.

For days with weak, discontinuous, or ambiguous modal evolution, the visual interpretation of the PNSD was further supported by the mean particle number concentrations in the 3–25 and 25–100 nm size ranges and candidate particle growth rates. These supporting parameters were used to improve the transparency and consistency of the day-by-day classification rather than as fixed classification thresholds.

Following this revision, 43 NPF days, 6 Undefined days, and 9 Non-Event days were identified during the 58 measurement days. The dates specifically mentioned by the referee, including 26 October 2024, 25 and 26 March 2025, and 10 and 19 October 2024, are now all included in the unified NPF-day category. Figures 2, 3, 5 – 7, and 10 and the corresponding statistical analyses have been revised using the new classification. Figures S1 – S3 now show the daily PNSDs for NPF, Undefined, and Non-Event days, respectively. In addition, Table S1 provides the revised day-by-day classification, NPF start

and end times, particle number characteristics, and candidate growth rates. The original growth subgroup is retained in Table S1 only for comparison and traceability and is not used in the revised main analyses.

Comment 2:

Particle formation rates J3 and J7 seem to have almost identical magnitude and diurnal variation (Fig 6) for Class I and Class II events. This would also support having only one NPF event class (combination of the Class I and Class II days).

Response 2：

Thank you for this observation. We agree that the similar magnitudes and diurnal variations of J_3 and J_7 for the former Class I and Class II events provide additional support for combining these two categories. Accordingly, we have removed the distinction between Class I and Class II and reclassified both categories as NPF days. Figure 6 and the corresponding text have also been revised based on the new three-category classification. Please see our Response 1 for further details regarding the revised classification.

Comment 3:

Have the authors compared the calculated CCN concentrations (calculated assuming const. hygroscopicity and supersaturation) to the measured accumulation mode number concetrations $N_{100-700}$, which is in many studies used as proxy for CCN? Based on Figures 5d and 10a, the diurnal variation of both these seems similar but the calculated CCN concentrations seem to be higher.

Response 3：

Thank you for this helpful suggestion. We have now directly compared the estimated CCN concentrations with $N_{100-700}$, which was obtained by integrating the measured PNSD over the 100–700 nm size range at the corresponding timestamps. The comparison is provided below as Fig. R1.

The estimated CCN concentrations were strongly correlated with $N_{100-700}$, with Spearman correlation coefficients of 0.91 during the autumn observation period (N=9665) and 0.82 during the spring observation period (N=8452). This result confirms that the two quantities exhibited broadly consistent temporal variability. However, as the reviewer correctly noted, the estimated CCN concentrations were systematically higher than $N_{100-700}$. The median CCN/$N_{100-700}$ ratios were 3.54 (interquartile range: 2.98–4.28) during the autumn observation period and 2.36 (1.88–2.90) during the spring observation period. The hourly median ratios also remained above unity throughout the day (Fig. R1).

This difference is expected because, under the assumed κ of 0.12 and supersaturation of 1.2%, the calculated critical activation diameter was approximately 43.45 nm. Therefore, the estimated CCN concentrations include potentially activatable particles between approximately 43 and 100 nm in addition to particles in the accumulation-mode size range. In contrast, $N_{100-700}$ excludes these potentially activatable Aitken-mode particles and consequently represents a more conservative proxy for CCN under the assumed conditions. We have clarified this distinction in Sect. 3.4 and emphasized

that the reported CCN concentrations are estimates based on the assumed hygroscopicity and supersaturation rather than direct CCN measurements.

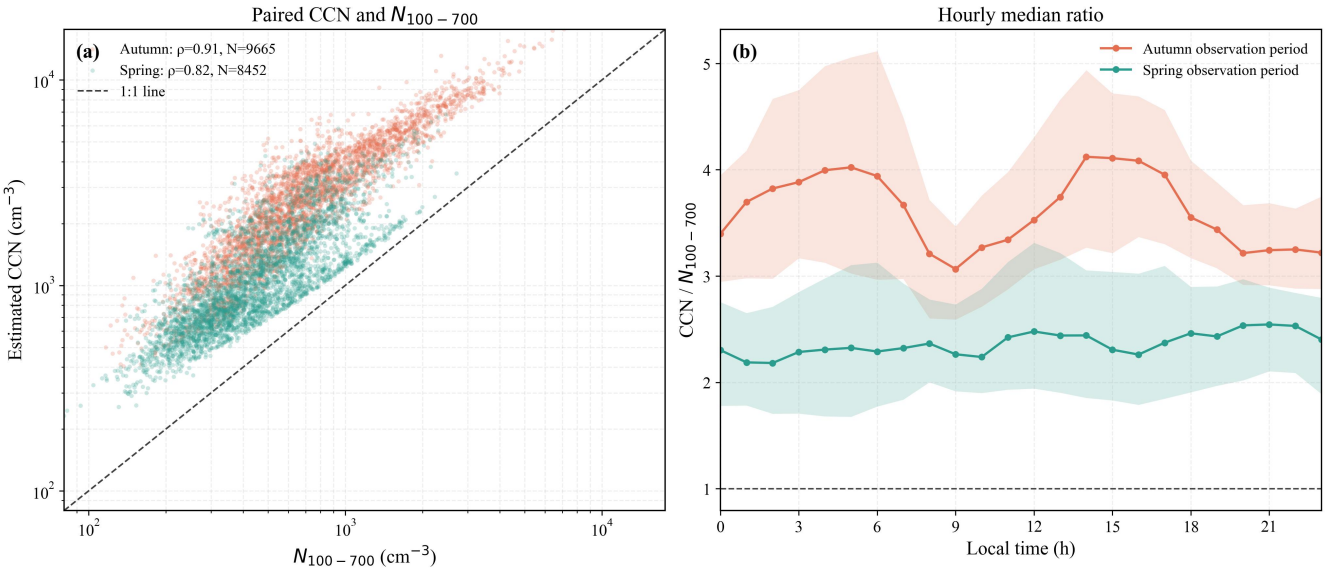

Figure R1. Comparison between estimated CCN concentrations and particle number concentrations in the 100–700 nm size range $N_{100–700}$ during the autumn and spring observation periods. (a) Paired estimated CCN and $N_{100–700}$ concentrations at corresponding timestamps. The dashed line denotes the 1:1 relationship, and ρ and N represent the Spearman correlation coefficient and number of valid paired observations, respectively. (b) Hourly median CCN/$N_{100-700}$ ratios; the shaded areas represent the interquartile ranges. CCN was estimated using (κ = 0.12) and a supersaturation of 1.2%.

Comment 4:

Please define all symbols used in Equations 6 and 7.

Response 4:

Thank you for pointing this out. We have revised the description following Eqs. (6) and (7) and now define all symbols used in these equations. The revised text reads:

CCN concentration is quantitatively calculated based on κ-Köhler theory (Petters and Kreidenweis, 2007). This method aims to determine the number of particles that can be activated at a specific supersaturation (S).

$$A = \frac{4\sigma_{s/a} M_w}{RT\rho_w} \tag{6}$$

$$\kappa = \frac{4A^3}{27 D_c^3 \ln^2 S_c} \tag{7}$$

In Eqs. (6) and (7), D_c is the critical dry particle diameter for CCN activation, S_c is the critical saturation ratio, and A is the Kelvin term. The parameter κ represents the influence of particle chemical composition on hygroscopicity and solution water activity. $\sigma_{s/a}$ is the surface tension of water against air. M_w and ρ_w are the molar mass and density of water, respectively. R is the universal gas constant, and T is the absolute temperature (K). In this study, κ and S were set to 0.12 and 1.2 %, respectively.

Table S1. Day-by-day revised classification, NPF timing, particle number characteristics, and candidate particle growth rates during the two observation periods. Mean $N_{3–25}$ and $N_{25–100}$ concentrations were calculated over 09:00–18:00 local time. Candidate $GR_{3–7}$ and $GR_{7–20}$ values were evaluated for every observation day by linear regression of automatically identified continuous modal trajectories. No R^2 threshold was applied. "NA" indicates that insufficient data or no sufficiently long and continuous trajectory was available.

Date	Revised classification	Original growth subgroup	NPF window	Mean $N_{3–25}$ (# cm^{-3})	Mean $N_{25–100}$ (# cm^{-3})	$GR_{3–7}$ window	$GR_{3–7}$ (nm h^{-1})	$GR_{7–20}$ window	$GR_{7–20}$ (nm h^{-1})
Oct 9, 2024	NPF day	Class II	8:40–14:30	16954	4977	08:42–09:12	4.26	09:17–14:27	1.62
Oct 10, 2024	NPF day	Class II	9:00–15:00	10803	4047	NA	NA	09:22–14:57	1.94
Oct 16, 2024	NPF day	Class I	9:00–21:00	19292	8532	09:02–09:32	3.90	09:37–17:57	0.93
Oct 17, 2024	NPF day	Class II	9:00–14:00	16605	5433	NA	NA	09:07–13:57	2.19
Oct 18, 2024	NPF day	Class II	8:40–14:30	16091	5005	08:42–09:27	3.47	09:32–14:27	1.35
Oct 19, 2024	NPF day	Class II	9:00–15:00	6346	3912	09:02–09:37	1.80	09:42–14:57	2.35
Oct 20, 2024	NPF day	Class II	9:00–18:00	21295	6244	09:02–13:07	0.17	09:42–17:52	1.30
Oct 22, 2024	NPF day	Class I	9:00–22:00	20350	6818	09:02–16:37	-0.02	09:37–17:57	-0.42
Oct 23, 2024	NPF day	Class II	9:00–15:00	12206	4174	NA	NA	09:02–14:57	0.93
Oct 24, 2024	NPF day	Class I	9:00–23:00	11971	4732	09:02–09:32	5.30	09:37–17:57	0.53
Oct 25, 2024	NPF day	Class I	9:00–21:00	11913	4686	09:02–09:47	3.60	09:52–17:57	1.21
Oct 26, 2024	NPF day	Class I	9:30–23:00	12083	3157	09:32–13:52	0.08	10:07–17:57	1.06
Oct 27, 2024	NPF day	Class I	9:30–22:00	15552	6391	NA	NA	09:47–17:57	1.28
Oct 28, 2024	NPF day	Class I	9:00–24:00	16668	5924	NA	NA	09:22–17:57	1.10
Oct 29, 2024	NPF day	Class I	9:30–24:00	10131	5355	NA	NA	09:47–17:57	1.43
Oct 30, 2024	NPF day	Class I	9:30–24:00	8331	4331	NA	NA	09:52–17:57	1.12
Oct 31, 2024	NPF day	Class I	9:30–21:00	9420	6128	NA	NA	10:02–17:57	0.78

Date	Revised classification	Original growth subgroup	NPF window	Mean $N_{3–25}$ (# cm^{-3})	Mean $N_{25–100}$ (# cm^{-3})	$GR_{3–7}$ window	$GR_{3–7}$ (nm h^{-1})	$GR_{7–20}$ window	$GR_{7–20}$ (nm h^{-1})
Nov 1, 2024	NPF day	Class I	9:30–24:00	18403	6892	NA	NA	10:02–17:57	0.85
Nov 2, 2024	NPF day	Class I	9:00–24:00	19211	7233	09:02–09:32	5.17	09:37–17:57	1.16
Nov 3, 2024	NPF day	Class I	9:00–21:00	14440	6669	09:02–09:52	3.13	09:57–17:57	1.31
Nov 4, 2024	NPF day	Class II	12:00–16:00	4937	3492	NA	NA	12:02–15:57	3.34
Nov 7, 2024	NPF day	Class I	9:00–24:00	24496	8216	NA	NA	09:27–17:57	0.49
Nov 8, 2024	NPF day	Class I	9:30–24:00	16717	8280	NA	NA	09:52–17:57	0.72
Nov 9, 2024	NPF day	Class I	9:30–24:00	14049	6956	NA	NA	09:42–17:57	1.08
Nov 10, 2024	NPF day	Class I	9:30–24:00	10546	5078	NA	NA	10:02–17:57	1.34
Mar 25, 2025	NPF day	Class I	9:00–21:00	13321	3237	NA	NA	09:25–18:00	1.05
Mar 26, 2025	NPF day	Class I	9:00–21:00	8415	3265	09:00–09:35	3.36	09:40–18:00	1.17
Mar 27, 2025	NPF day	Class II	9:00–17:00	15776	3581	NA	NA	09:20–17:00	0.60
Mar 28, 2025	NPF day	Class II	9:00–14:00	12317	2713	NA	NA	09:20–13:40	2.22
Mar 30, 2025	NPF day	Class II	9:00–11:00	3715	561	09:00–09:35	4.33	09:40–10:55	4.73
Apr 2, 2025	NPF day	Class II	8:30–12:30	7511	1182	08:30–09:35	1.67	09:40–12:30	1.49
Apr 6, 2025	NPF day	Class II	8:30–13:00	13406	1586	NA	NA	08:30–12:55	0.98
Apr 7, 2025	NPF day	Class II	8:30–12:30	8616	2079	08:30–09:00	5.78	09:05–12:25	2.16
Apr 8, 2025	NPF day	Class II	8:30–16:30	9734	1750	08:30–09:10	3.92	09:15–16:25	0.95
Apr 9, 2025	NPF day	Class II	9:00–16:00	6494	3110	09:00–09:35	3.48	09:40–15:55	1.60
Apr 12, 2025	NPF day	Undefined	9:00–11:00	4131	2176	NA	NA	09:20–10:55	8.44
Apr 13, 2025	NPF day	Class II	9:00–16:00	9928	2010	09:00–09:40	3.51	09:45–15:55	1.22
Apr 16, 2025	NPF day	Class II	8:30–16:00	11387	5571	NA	NA	09:00–15:55	1.28
Apr 17, 2025	NPF day	Class I	8:00–18:00	16775	6852	NA	NA	08:30–17:55	1.03

Date	Revised classification	Original growth subgroup	NPF window	Mean $N_{3–25}$ (# cm^{-3})	Mean $N_{25–100}$ (# cm^{-3})	$GR_{3–7}$ window	$GR_{3–7}$ (nm h^{-1})	$GR_{7–20}$ window	$GR_{7–20}$ (nm h^{-1})
Apr 18, 2025	NPF day	Undefined	11:00–14:00	5239	1392	NA	NA	11:25–13:55	1.59
Apr 19, 2025	NPF day	Class II	8:30–18:00	10978	3950	NA	NA	08:50–17:55	1.15
Apr 21, 2025	NPF day	Class I	8:00–21:00	15983	4139	08:00–08:30	2.95	08:35–17:55	0.93
Apr 22, 2025	NPF day	Class II	9:00–16:00	9488	1375	NA	NA	09:15–15:55	0.46
Oct 15, 2024	Undefined	Undefined	NA	2042	1142	07:17–12:57	-0.14	07:02–17:57	0.44
Mar 29, 2025	Undefined	Undefined	NA	2946	644	13:35–14:25	0.67	07:00–17:55	-0.28
Apr 10, 2025	Undefined	Undefined	NA	3888	819	NA	NA	07:00–17:55	-0.05
Apr 11, 2025	Undefined	Undefined	NA	5214	989	NA	NA	07:00–17:45	-0.02
Apr 14, 2025	Undefined	Undefined	NA	2597	1219	NA	NA	07:05–17:55	0.60
Apr 20, 2025	Undefined	Undefined	NA	4855	873	NA	NA	07:20–17:55	0.40
Oct 21, 2024	Non-Event	Non-Event	NA	2011	1117	12:32–13:42	-0.72	07:02–17:57	0.39
Nov 5, 2024	Non-Event	Non-Event	NA	1034	2292	07:12–17:57	-0.25	07:02–17:17	0.80
Nov 6, 2024	Non-Event	Non-Event	NA	1085	2751	NA	NA	07:02–17:57	-0.35
Mar 31, 2025	Non-Event	Non-Event	NA	517	366	14:35–17:00	0.07	07:00–17:15	-0.88
Apr 1, 2025	Non-Event	Non-Event	NA	170	410	13:50–14:25	0.52	14:30–18:00	0.49
Apr 3, 2025	Non-Event	Non-Event	NA	688	401	07:35–10:55	-0.19	07:00–18:00	-0.15
Apr 4, 2025	Non-Event	Non-Event	NA	245	443	NA	NA	07:20–18:00	-0.01
Apr 5, 2025	Non-Event	Non-Event	NA	254	585	NA	NA	07:00–17:55	0.16
Apr 15, 2025	Non-Event	Non-Event	NA	846	1023	NA	NA	07:00–17:35	-0.37

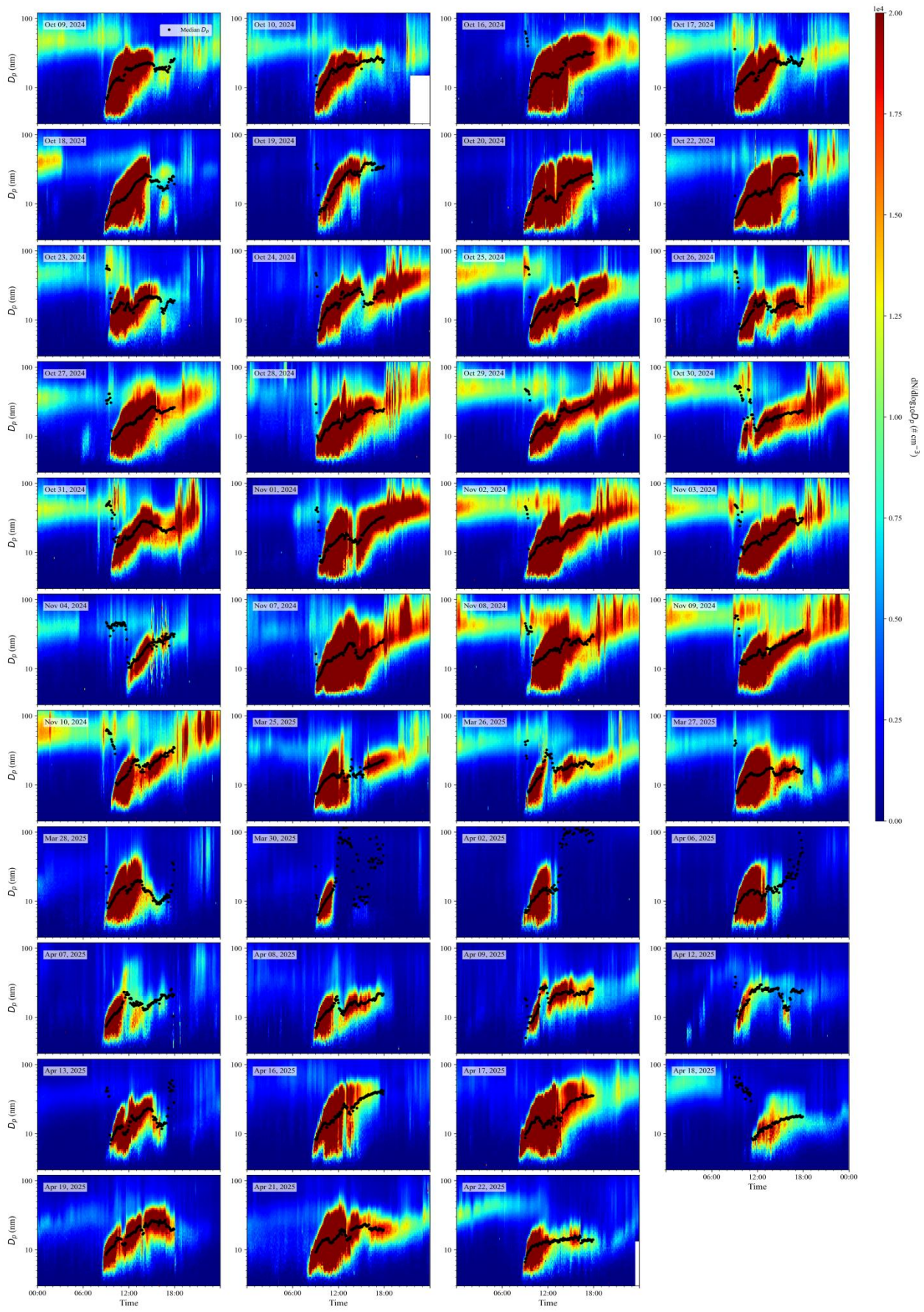

Figure S1: PNSDs for all NPF days. Each panel represents one day. The black dots indicate the median particle diameter.

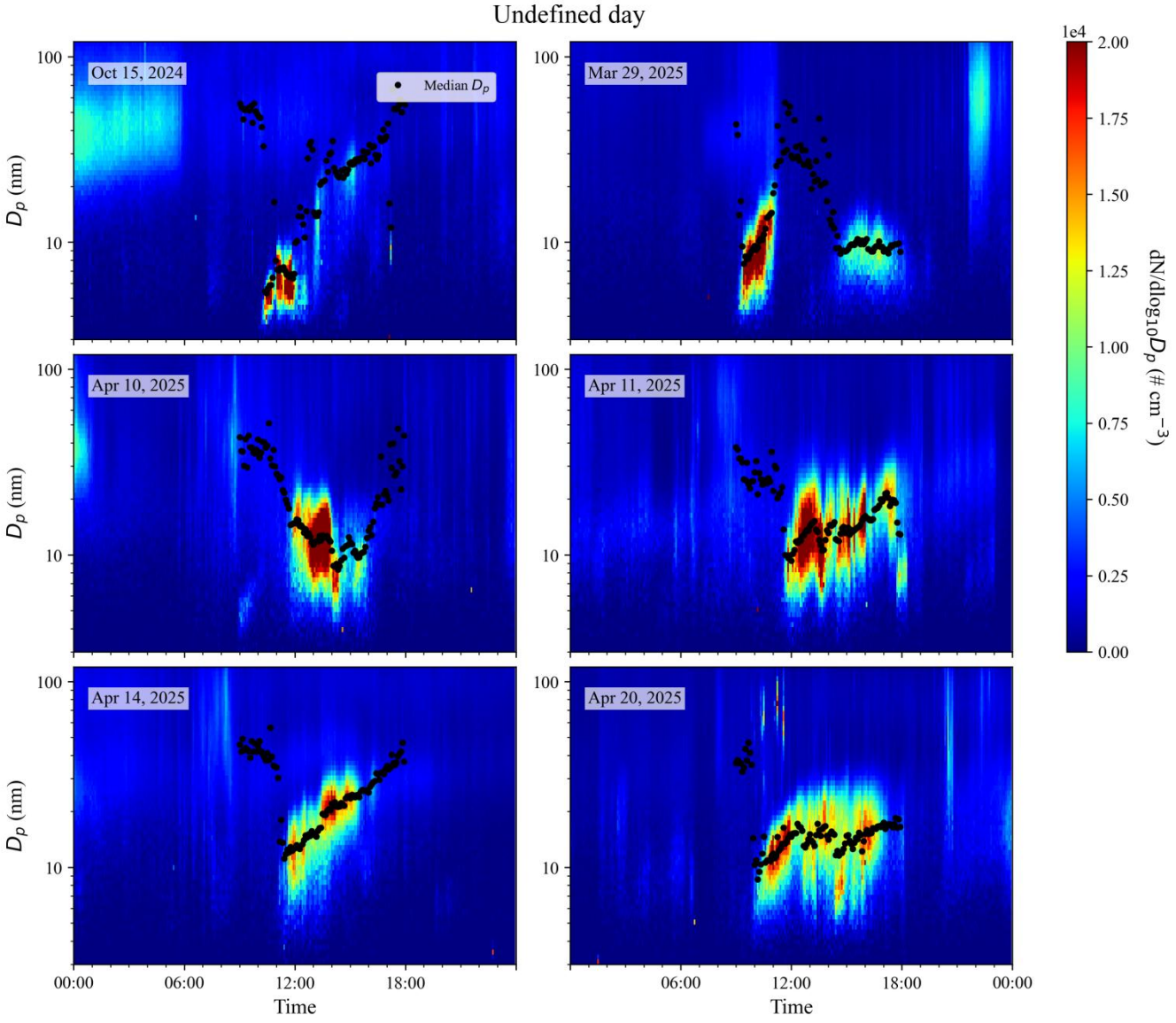

Figure S2: PNSDs for all Undefined days. Each panel represents one day. The black dots indicate the median particle diameter.

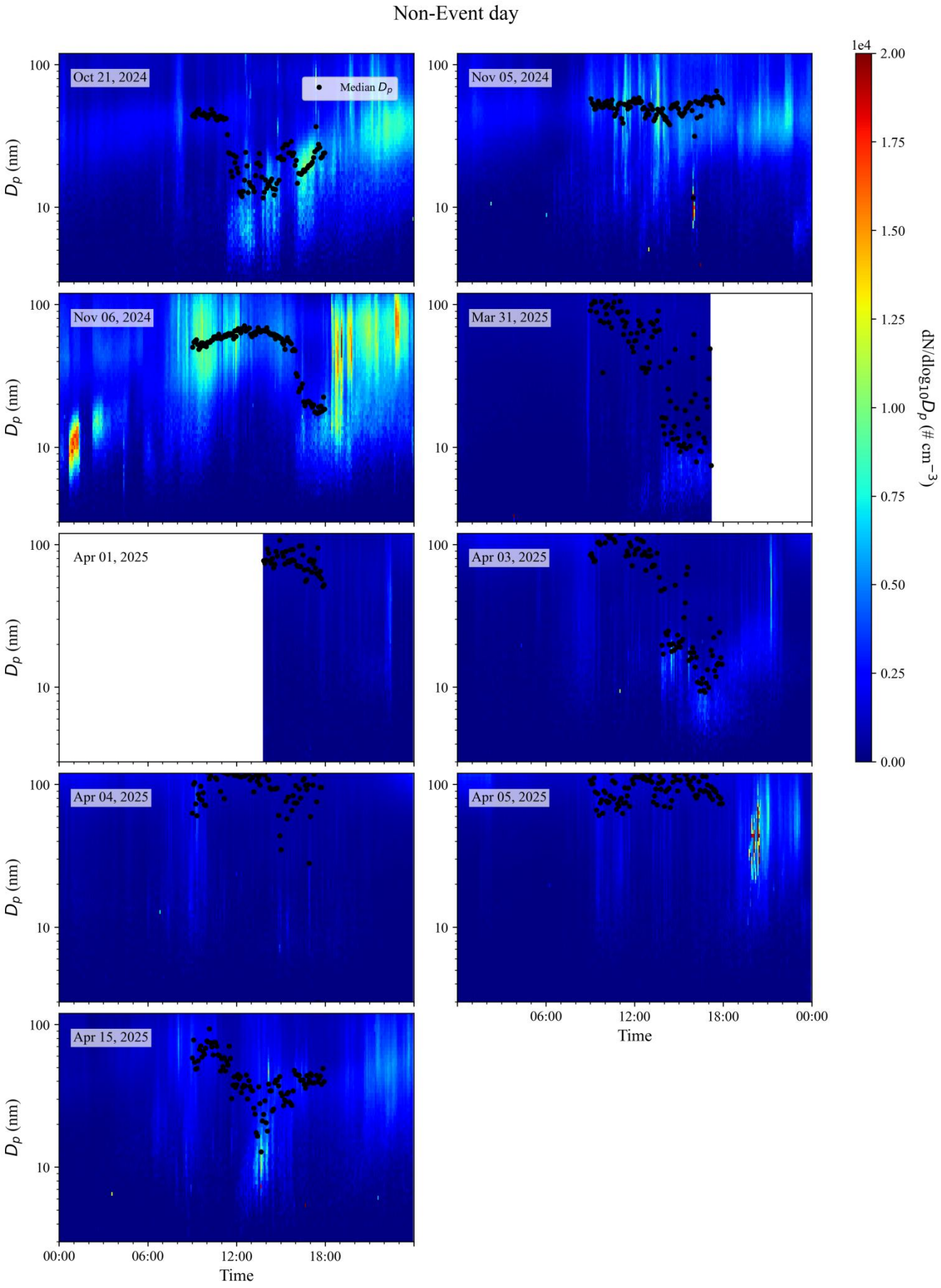

Figure S3: PNSDs for all Non-Event days. Each panel represents one day. The black dots indicate the median particle diameter.